Engineering xxx (xxxx) xxx

Contents lists available at ScienceDirect

Engineering

journal homepage: www.elsevier.com/locate/eng

Research
Microecology—Article

Altered Tongue Coating Microbiota Drives Intestinal Inflammation in Patients with Inflammatory Bowel Disease

Yanqing Wang [a,#], Qian Xu [b,#], Jingyuan Wang [d,#], Meng Xue [d], Honghong Liu [a], Yifei Yang [e], Chao Ye [c], Shuling Wang [f], Gerong Zhang [g], Wenrui Guo [d], Wei Jiang [d], Eran Elinav [h,i], Shu Zhu [c,d,*], Guorong Zhang [c,d,*]

[a] *Department of Stomatology, The First Affiliated Hospital of University of Science and Technology of China, Division of Life Sciences and Medicine, University of Science and Technology of China, Hefei 230001, China*
[b] *Department of Anhui Provincial Clinical Laboratory Centre, Centre for Leading Medicine and Advanced Technologies of Institute of Health and Medcine, The First Affiliated Hospital of University of Science and Technology of China, Division of Life Sciences and Medicine, University of Science and Technology of China, Hefei 230001, China*
[c] *Department of Digestive Disease, The First Affiliated Hospital of University of Science and Technology of China, Division of Life Sciences and Medicine, University of Science and Technology of China, Hefei 230001, China*
[d] *Key Laboratory of Immune Response and Immunotherapy, School of Basic Medical Sciences, Division of Life Sciences and Medicine, University of Science and Technology of China, Hefei 230001, China*
[e] *School of Artificial Intelligence and Data Science, University of Science and Technology of China, Hefei 230001, China*
[f] *National Clinical Research Center for Digestive Diseases, Department of Gastroenterology, Changhai Hospital, Naval Medical University, Shanghai 200433, China*
[g] *Department of Molecular & Cell Biology, University of California, Berkeley, CA 94720, USA*
[h] *Systems Immunology Department, Weizmann Institute of Science, Rehovot 76100, Israel*
[i] *Microbiome & Cancer Division, German Cancer Research Center (DKFZ), Heidelberg 69120, Germany*

ARTICLE INFO

Article history:
Received 2 April 2025
Revised 2 December 2025
Accepted 3 February 2026
Available online xxxx

Keywords:
Tongue coating microbiota
Inflammatory bowel disease (IBD)
Oral–gut axis
Microbiota transplantation

ABSTRACT

Emerging evidence highlights the oral–gut axis as an important contributor to the pathogenesis of inflammatory bowel disease (IBD); however, the specific role of the tongue coating microbiota remains poorly understood. To comprehensively delineate oral–gut microbial alterations in IBD, we analyzed tongue coating and fecal microbiota from 596 participants, including 278 patients with Crohn's disease (CD), 91 with ulcerative colitis (UC), and 227 healthy controls (HCs), using 16S ribosomal RNA (rRNA) gene sequencing. Patients with IBD exhibited a distinct dysbiotic signature in tongue coating microbiota, characterized by increased abundances of *Streptococcus*, *Prevotella*, and *Gemella* in both CD and UC patients, alongside a CD-specific depletion of commensal taxa such as *Neisseria* and *Fusobacterium* compared with HCs. Notably, a similar oral microbial shift was observed in a spontaneous enteritis mouse model, which demonstrated enrichment of oral *Streptococcus* and concordant increases in *Prevotella* across both oral and intestinal niches. To establish causality, tongue coating microbiota from CD patients were transplanted into antibiotic-pretreated mice, resulting in significantly exacerbated colitis relative to recipients of HC-derived microbiota. Mechanistically, *Streptococcus* strains isolated from CD patients promoted Th1 cell polarization *in vitro* and aggravated colitis *in vivo*, implicating these orally derived pathobionts in the amplification of intestinal inflammation. Together, these findings identify the tongue coating microbiota as a previously underappreciated mediator of gut inflammation in IBD, support its potential utility as a non-invasive biomarker for CD, and provide mechanistic evidence that oral microbial dysbiosis can actively drive intestinal immune pathology.

1. Introduction

Inflammatory bowel disease (IBD), encompassing Crohn's disease (CD) and ulcerative colitis (UC), comprises chronic,

* Corresponding authors.
E-mail addresses: zhushu@ustc.edu.cn (S. Zhu), zhgr@ustc.edu.cn (G. Zhang).
# These authors contributed equally to this work.

https://doi.org/10.1016/j.eng.2026.02.016
2095-8099/

Please cite this article as: Y. Wang, Q. Xu, J. Wang et al., Altered Tongue Coating Microbiota Drives Intestinal Inflammation in Patients with Inflammatory Bowel Disease, Engineering, https://doi.org/10.1016/j.eng.2026.02.016

relapsing inflammatory disorders of the gastrointestinal tract with complex and incompletely understood etiologies [1]. The global prevalence of IBD has risen steadily over recent decades, imposing a substantial and growing burden on healthcare systems worldwide [2–4]. Clinically, IBD is characterized by a fluctuating course of remission and relapse, with disease flares commonly presenting as hematochezia, abdominal pain, diarrhea, and fever, along with a broad spectrum of extraintestinal manifestations (EIMs), including arthritis, uveitis, dermatologic and oral mucosal lesions, hepatobiliary disease, and osteoporosis [5,6].

Although the precise mechanisms driving IBD remain elusive, accumulating evidence implicates intestinal microbial dysbiosis as a central contributor to disease pathogenesis [7–9]. This dysbiosis is typically marked by reduced microbial diversity, loss of beneficial commensals, and expansion of pro-inflammatory pathobionts. Advances in next-generation sequencing have revealed profound alterations in gut microbial composition in patients with IBD [10,11]. However, whether these microbial shifts represent a primary cause of intestinal inflammation or arise as a consequence of mucosal injury and immune dysregulation remains an area of active investigation [12]. Beyond the gut microbiome, increasing attention has been directed toward the role of the oral microbiota as a potential upstream regulator of intestinal inflammation. The oral cavity harbors one of the most diverse microbial communities in the human body and serves as a continuous source of microbes that are swallowed and introduced into the gastrointestinal tract. The concept of the oral-gut axis has thus emerged as a critical framework for understanding bidirectional microbial and immunological interactions between these two compartments [13]. Oral microbial dysbiosis and translocation have been implicated in a range of systemic diseases, including diabetes, cardiovascular disease, and gastric cancer [14–16]. In IBD, recent studies suggest that oral-derived pathobionts can ectopically colonize the intestine, disrupt mucosal homeostasis, and exacerbate intestinal inflammation [17,18].

The tongue coating represents a distinct, relatively stable, and easily accessible microbial niche within the oral cavity. It consists of a complex matrix of bacteria, desquamated epithelial cells, salivary components, and dietary residues [19,20], and may reflect both local oral conditions and systemic inflammatory states. Clinical observations have reported thicker tongue coatings in patients with IBD, raising the possibility that alterations in tongue coating microbiota are related to intestinal inflammation [20,21]. Despite its potential diagnostic and mechanistic relevance, the composition and functional significance of tongue coating microbiota in IBD remain largely unexplored.

In this study, we sought to systematically characterize the tongue coating microbiota in patients with IBD and to elucidate its contribution to intestinal inflammation. By integrating large-scale human cohort analyses with complementary murine models, we identified a distinct dysbiotic signature in the tongue coating of IBD patients, characterized by enrichment of *Streptococcus*, *Prevotella*, and *Gemella*. This oral microbial profile was recapitulated in a spontaneous enteritis mouse model. Importantly, transplantation of tongue coating microbiota from patients with CD into antibiotic-pretreated mice exacerbated colitis, establishing a causal role for disease-associated oral microbiota in driving gut inflammation. Mechanistic studies further demonstrated that oral-derived *Streptococcus* strains promote Th1 polarization and aggravate intestinal pathology. Collectively, these findings identify the tongue coating microbiota as a reservoir of pro-inflammatory pathobionts and highlight its potential utility as a non-invasive biomarker for CD, providing new insights into the pathogenic relevance of the oral–gut axis in IBD.

2. Material and methods

2.1. Patients

Tongue coating and fecal samples were collected from participants recruited at the Department of Digestive Diseases, The First Affiliated Hospital of the University of Science and Technology of China (USTC), between December 2020 and December 2022. The study protocol was approved by the Ethics and Investigation Committee of the First Affiliated Hospital of USTC (approval No. 2021KY02), and written informed consent was obtained from all participants prior to enrollment.

Hospitalized patients with a clinical diagnosis of IBD were eligible for inclusion if they had not received antibiotics or traditional Chinese medicine within seven days before sample collection. Diagnoses of UC and CD were established in accordance with the 2010 World Gastroenterology Organization Practice Guidelines and the ECCO–ESGAR consensus guidelines for the diagnosis and management of IBD [5,22]. These guidelines integrate clinical presentation, endoscopic findings, radiologic assessment, and histopathological evaluation to ensure standardized and evidence-based disease classification.

Demographic characteristics, disease phenotype and duration, clinical symptoms, EIMs, coexisting primary sclerosing cholangitis, and medication histories were extracted from electronic medical records. Patients with a history of surgical resection for intestinal lesions were excluded. Disease activity was assessed using the partial Mayo score for UC and the short Crohn's disease activity index (sCDAI) for CD. Clinical remission was defined as a partial Mayo score ≤ 2 for UC and an sCDAI ≤ 4 for CD. Healthy controls (HCs) were recruited from individuals undergoing routine health examinations. Participants with a history of chronic metabolic or inflammatory diseases (including diabetes, hypertension, and hyperlipidemia) were excluded. Absence of IBD was confirmed by baseline endoscopic and histopathological evaluations.

2.2. Sample collection

Participants were instructed to refrain from tooth brushing on the night before tongue coating sample collection. On the morning of sampling, prior to oral hygiene, tongue coating was gently scraped from approximately two-thirds of the central and anterior regions of the tongue using sterile instruments. Samples were immediately suspended in an equal volume of phosphate-buffered saline (PBS) containing 20% (w/v) glycerol, snap-frozen in liquid nitrogen, and stored at −80 °C until further analysis. Fecal samples were collected from the same participants on the day of tongue coating sampling and processed using identical cryopreservation procedures. Comprehensive clinical data were recorded for all participants, and all sample collections were conducted on a voluntary basis.

2.3. Animals

All animal experiments were performed using age- and sex-matched C57BL/6 mice (6–10 weeks old) obtained from Gempharmatech Co., Ltd. (China). C57BL/6-TNF$^{\Delta ARE}$ mice (TNF: tumor necrosis factor; ARE: AU-rich element) and their wild-type (WT) littermate controls were used as previously described [23]. Mice were maintained under specific pathogen-free conditions with a 12-hour light–dark cycle (lights on from 08:00 to 20:00), controlled temperature and humidity, with *ad libitum* access to food and water. All animal procedures were approved by the Ethics Committee of USTC (approval No. 2024-N(A)-114) and conducted in accordance with institutional and national guidelines.

2.4. Tongue coating microbiota transplantation

Tongue coating microbiota transplantation was performed as previously described with minor modifications [24]. Fresh tongue coating samples from patients with CD or HCs were resuspended in sterile PBS under anaerobic conditions with vigorous agitation and allowed to settle for 2 min. The supernatant containing microbial suspensions was collected and immediately administered to recipient mice. To deplete endogenous commensal microbiota, recipient mice were treated with a broad-spectrum antibiotic cocktail (ampicillin 1 $g{\cdot}L^{-1}$, neomycin sulfate 1 $g{\cdot}L^{-1}$, metronidazole 1 $g{\cdot}L^{-1}$, and vancomycin 0.5 $g{\cdot}L^{-1}$; Sangon Biotech (Shanghai) Co., Ltd., China) in drinking water for seven consecutive days prior to transplantation. Two weeks after microbiota transplantation, experimental colitis was induced by administration of dextran sodium sulfate (DSS) in the drinking water.

2.5. DSS-induced colitis

Experimental colitis was induced by administering 2.5% (w/v) DSS (MP Biomedicals, USA) in the drinking water for two consecutive days, followed by replacement with regular drinking water until the end of the experiment. Mice were monitored daily for changes in body weight and clinical signs of colitis. At sacrifice, colons were excised and measured to assess disease severity.

2.6. 2,4,6-Trinitrobenzene sulfonic acid (TNBS)-induced colitis

TNBS-induced colitis was established as previously described with minor modifications [25]. Briefly, mice were presensitized by shaving a 1.5 cm × 1.5 cm area of dorsal skin between the scapulae and topically applying 150 μL of TNBS presensitization solution. This solution was prepared by vortexing acetone (Sangon Biotech (Shanghai) Co., Ltd.) and olive oil (MedChemExpress, USA) at a 4:1 (v/v) ratio, followed by mixing four volumes of this solvent with one volume of 5% (w/v) TNBS (Sigma, Germany) to achieve a final TNBS concentration of 1% (w/v). Control mice received an identical vehicle solution lacking TNBS. Seven days after presensitization, mice were weighed, anesthetized, and administered 100 μL of TNBS solution into the colonic lumen using a 3.5-French catheter inserted approximately 4 cm proximal to the anus. The TNBS enema solution was prepared by mixing equal volumes of 5% (w/v) TNBS in water and absolute ethanol. Following instillation, mice were maintained in a vertical, head-down position for 60 s to ensure retention of the solution before recovery.

2.7. Bacterial isolation and culture

Bacterial isolation was performed as previously described [26]. Tongue coating samples from patients with CD were serially diluted in sterile PBS (10^{-1} to 10^{-4}) and plated onto non-selective Gifu anaerobic medium (GAM) agar (Solarbio, China). Plates were incubated under anaerobic conditions (80% N_2, 10% H_2, 10% CO_2) in an anaerobic chamber (Electrotek, UK) at 37 °C for 2–4 d. Individual colonies were picked and identified by amplification and sequencing of the 16S rRNA gene using universal primers (27F: 5′-AGRGTTTGATYMTGGCTCAG-3′, 1492R: 5′-GGYTACCTTGTTACGACTT-3′). Resulting sequences were compared against the National Center for Biotechnology Information (NCBI) database for taxonomic assignment. For bacterial administration, individual strains were cultured in GAM broth (Solarbio), harvested during the logarithmic growth phase, and orally gavaged into antibiotic-pretreated mice at approximately 1×10^8 CFU per strain in 200 μL sterile PBS per mouse. For preparation of heat-killed bacteria, *Streptococcus* strains were cultured twice with sterile PBS, and heat-inactivated at 121 °C for 30 min.

2.8. In vitro T cell differentiation

Naïve cluster of differentiation 4 positive ($CD4^+$) T cells were isolated from mouse spleens using a $CD4^+$ naïve T cell isolation kit (BioLegend, USA) according to the manufacturer's instructions [27,28]. Cells were seeded at equal densities into 96-well plates pre-coated with anti-CD3 antibody (2 $\mu g{\cdot}mL^{-1}$; BioLegend) and stimulated in the presence of bacterial culture supernatants or control media (pH adjusted to 7.0) at a final concentration of 2.5% (v/v), or with heat-killed bacteria at a 1:1 cell-to-bacteria ratio. For Th17 differentiation, cultures were supplemented with anti-CD28 monoclonal antibody (1 $\mu g{\cdot}mL^{-1}$; BioLegend), mouse interleukin (IL)-6 (25 $ng{\cdot}mL^{-1}$; BioLegend), mouse IL-23 (20 $ng{\cdot}mL^{-1}$; BioLegend), human transforming growth factor-β1 (TGF-β1; 2 $ng{\cdot}mL^{-1}$; BioLegend), anti-mouse interferon-γ (IFN-γ; 5 $\mu g{\cdot}mL^{-1}$; BioLegend), and anti-mouse IL-4 (5 $\mu g{\cdot}mL^{-1}$; BioLegend). For Th1 differentiation, cultures received anti-CD28 (1 $\mu g{\cdot}mL^{-1}$), human IL-2 (50 $U{\cdot}mL^{-1}$; BioLegend), mouse IL-12 (20 $ng{\cdot}mL^{-1}$; BioLegend), and anti-mouse IL-4 (5 $\mu g{\cdot}mL^{-1}$). Cells were cultured at 37 °C in a humidified incubator with 5% CO_2 for 4 d. Following stimulation, cells were harvested and intracellular IFN-γ and IL-17A expression was analyzed by flow cytometry.

2.9. Isolation of lamina propria lymphocytes (LPLs)

LPLs were isolated from colonic tissues immediately following euthanasia. Excised colons were flushed with ice-cold PBS (KeyGEN BioTECH, China), opened longitudinally, and subjected to two sequential 30-min incubations in PBS supplemented with 2 $mmol{\cdot}L^{-1}$ ethylenediaminetetraacetic acid (EDTA; Sangon Biotech (Shanghai) Co., Ltd.) and 2% fetal bovine serum (FBS; VivaCell, China) at 37 °C with constant shaking at 250 rpm to remove epithelial cells. Tissues were then extensively washed with PBS to eliminate residual EDTA. Subsequently, colonic tissues were minced into fragments < 5 mm in size and enzymatically digested for 30 min at 37 °C in Roswell Park Memorial Institute (RPMI)-1640 medium (KeyGEN BioTECH) containing 0.5 $mg{\cdot}mL^{-1}$ collagenase type II (Sigma), 0.5 $mg{\cdot}mL^{-1}$ DNase I (Sigma), and 2% FBS, with continuous agitation at 250 rpm. The resulting cell suspension was filtered through a 70-μm nylon mesh, washed twice with PBS containing 2% FBS, and resuspended in complete RPMI-1640 medium supplemented with 10% FBS and 1% penicillin–streptomycin. Cell viability consistently exceeded 95%, as assessed by trypan blue exclusion [27]. Isolated cells were immediately processed for downstream analyses.

2.10. Flow cytometry analysis

Single-cell suspensions were incubated with fluorochrome-conjugated monoclonal antibodies (BioLegend) diluted in PBS containing 0.5% FBS and 2 $mmol{\cdot}L^{-1}$ EDTA for 20 min at 4 °C in the dark for surface marker staining. For intracellular cytokine detection, cells were stimulated for 4 h in RPMI-1640 supplemented with 10% FBS and Cell Stimulation Cocktail (1:500 dilution; eBioscience, USA), according to the manufacturer's instructions. Following stimulation, 1×10^6 cells were fixed and permeabilized using the BD Cytofix/Cytoperm™ kit (BD Biosciences, USA) for 20 min at 4 °C, followed by intracellular staining with cytokine-specific antibodies as per the manufacturer's protocol. Cells were washed with Perm/Wash buffer (BD Biosciences), resuspended in magnetic-activated cell sorting (MACS) buffer (PBS containing 0.5% FBS and 2 $mmol{\cdot}L^{-1}$ EDTA), and analyzed on a CytoFLEX S flow cytometer (Beckman Coulter, USA). Data acquisition and analysis were performed using FlowJo™ software v10.8 (BD Life Sciences, USA). Gating strategies were standardized across experiments, and all antibodies were validated for specificity and used at a dilution of

1:200 unless otherwise indicated. The following antibody conjugates were used: CD45.2-APC/Cy7 (clone 104), CD3-FITC (clone 17A2), CD4-Super Bright 600 (clone RM4-5), IL-17A-PE (clone TC11-18H10.1), and IFN-γ-PE/Cy7 (clone XMG1.2). Cell viability was assessed using 4′,6-diamidino-2-phenylindole (DAPI) (BioLegend) and MitoTracker™ Deep Red FM dye (Thermo Fisher Scientific, USA).

2.11. Histological analysis

Distal colon segments from colitis model mice were fixed in 4% paraformaldehyde (PFA) and cryoprotected through a graded sucrose series (10%, 20%, and 30%). For each sample, four transverse sections representing distinct anatomical regions were prepared and stained with hematoxylin and eosin (H&E) according to standard protocols. Histological evaluation was performed in a blinded manner using established scoring criteria encompassing three parameters: ulceration severity (0, absent; 1, punctate; 2, minimal; 3, moderate; 4, extensive), inflammatory cell infiltration (0, none; 1, minimal; 2, mild; 3, moderate; 4, severe), and depth of inflammation (0, none; 1, mucosal; 2, mucosal and submucosal; 3, transmural; 4, full-thickness) [29]. The cumulative histological score for each animal was calculated by summing the scores of these parameters across three randomly selected sections.

2.12. 16S rRNA gene sequencing and microbiota analysis

All samples were stored at −80 °C until processing. Genomic DNA was extracted from tongue coating, intestinal mucus, and fecal samples using the QIAamp Fast DNA Stool Mini Kit (Cat. No. 51604; QIAGEN, Germany) according to the manufacturer's protocol. The V4 hypervariable region of the bacterial 16S rRNA gene was amplified using the primer pair 515F/806R, as recommended by the Earth Microbiome Project 2. The barcoded forward primer sequence was 515F: AATGATACGGCGACCACCGAGATCTACACGCT XXXXXXXXXXXXTATGGTAATTGTGTGYCAGCMGCCGCGGTAA, and the reverse primer sequence was 806R: CAAGCAGAAGACGGCAT ACGAGATAGTCAGCCAGCCGGACTACNVGGGTWTCTAAT. Amplicons were quantified, pooled at equimolar concentrations, purified using the QIAquick PCR Purification Kit (Cat. No. 28104; QIAGEN), and sequenced on an Illumina MiSeq platform using the v3 kit with 250-bp paired-end reads. Sequencing yielded an average depth of 29 292 ± 11 228 reads per sample (mean ± standard deviation (SD)). Raw sequencing data were processed using a customized bioinformatics pipeline integrating USEARCH (v8.1), VSEARCH (v2.13.0), and QIIME (v1.9.1). Quality filtering, chimera removal, and clustering were performed to generate an operational taxonomic unit (OTU) table. Taxonomic assignment was conducted using the Ribosomal Database Project (RDP) classifier. For β-diversity analyses, unweighted UniFrac distances were calculated and visualized by principal coordinates analysis (PCoA) based on a rarefaction depth of 5000 reads per sample. Statistical differences in microbial community structure among groups were assessed using permutational multivariate analysis of variance (PERMANOVA) implemented in the vegan package (v2.5-7) in R (v4.0.5).

2.13. Accession numbers

The 16S rRNA gene sequencing datasets have been deposited in the NCBI Sequence Read Archive (SRA) under BioProject accession numbers PRJNA1103394, PRJNA1103950, and PRJNA1102901.

3. Results

3.1. Distinct microbial profiles in oral and fecal microbiota of patients with IBD

A total of 596 participants were included in the study, comprising 91 patients with UC (68 active and 23 in remission), 278 patients with CD (145 active and 133 in remission), and 227 HCs (Table 1).

We analyzed 16S rRNA sequencing data from 414 tongue coating samples (195 HCs, 173 CD, and 46 UC) and 81 fecal samples (9 HCs, 47 CD, and 25 UC). PCoA based on unweighted UniFrac distances revealed a significant separation of tongue coating microbial communities between CD patients and HCs (PERMANOVA, CD vs HC: P = 0.001), whereas no significant difference was observed between UC patients and HCs (UC vs HC: P = 0.168; Fig. 1(a)). Consistent with these findings, CD patients exhibited a significant reduction in α-diversity compared with HCs (Figs. 1(b) and (c)). At the genus level, both CD and UC patients showed a marked enrichment of *Streptococcus* in the tongue coating relative to HCs (Figs. 1(d) and (e)). *Prevotella* was also significantly increased in CD patients. Further differential abundance analyses identified enrichment of *Gemella* and concomitant depletion of commensal genera, including *Fusobacterium* and *Neisseria*, specifically in the tongue coating of CD patients (Figs. 1(f) and (g)). In UC patients, elevated abundances of select *Prevotella* species and *Gemella* were similarly observed (Figs. 1(f) and (h)). Collectively, these results demonstrate that IBD, particularly CD, is associated with a distinct dysbiotic signature in tongue coating microbiota, characterized by expansion of oral-associated genera such as *Streptococcus*, *Prevotella*, and *Gemella*. The consistent enrichment of these taxa suggests a potential role for tongue-derived oral pathobionts in amplifying mucosal immune responses and contributing to intestinal inflammation.

PCoA of fecal microbiota based on Bray–Curtis dissimilarity revealed clear separation among CD, UC, and HC groups (PERMA-

Table 1
Demographic characteristics of HCs and IBD patients.

Characteristics	UC (N = 91)	CD (N = 278)	HCs (N = 227)	Total (N = 596)	P-value
Age					3.80×10^{-10}
Mean ± SD	39.12 ± 13.28	30.59 ± 10.45	34.11 ± 9.59	33.14 ± 11.17	—
Median	40.00	30.00	32.00	31.00	—
{min, max}	{14.00, 61.00}	{14.00, 61.00}	{18.00, 58.00}	{14.00, 61.00}	—
Gender					1.90×10^{-12}
Female	35 (38.46%)	64 (23.02%)	121 (53.30%)	220 (36.91%)	—
Male	56 (61.54%)	214 (76.98%)	106 (46.70%)	376 (63.09%)	—
Stage (UC)					
UC-active	68 (74.73%)	0	0	68 (11.41%)	—
UC-remission	23 (25.27%)	0	0	23 (3.86%)	—
Stage (CD)					
CD-active	0	145 (52.16%)	0	145 (24.33%)	—
CD-remission	0	133 (47.84%)	0	133 (22.32%)	—

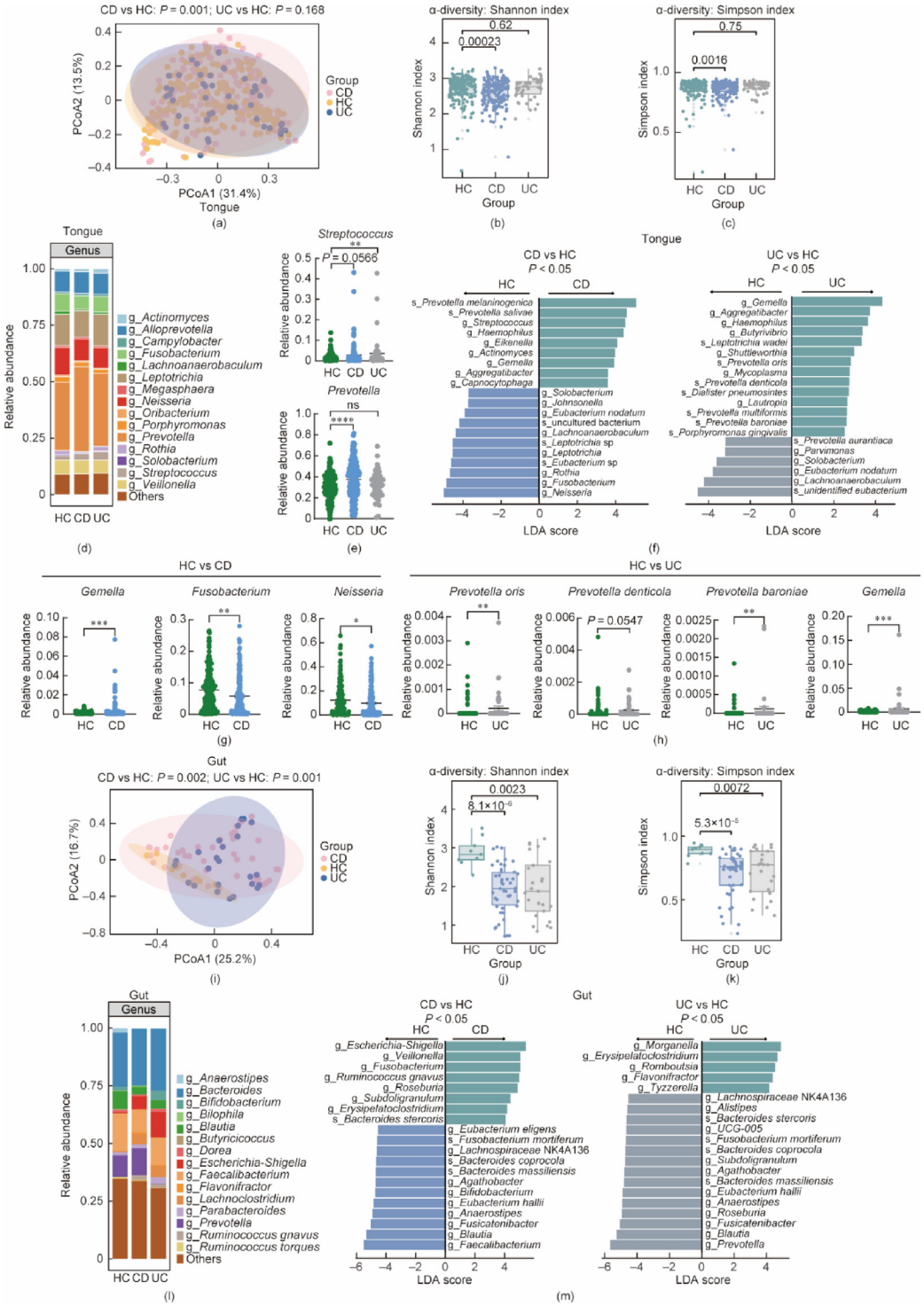

Fig. 1. Characteristics of tongue coating and gut microbiota in patients with IBD. (a–h) Tongue coating microbiota analysis. (a) PCoA based on Bray–Curtis dissimilarity showing β-diversity of tongue coating samples. Each point represents an individual sample. Differences in microbial composition among groups were assessed by PERMANOVA ($P < 0.05$). (b, c) α-Diversity of tongue coating microbiota assessed using the (b) Shannon and (c) Simpson indices. One-way analysis of variance (ANOVA) indicated significant differences among groups ($P < 0.05$). The center line denotes the median, boxes represent the interquartile range (IQR), whiskers extend to 1.5× IQR, and outliers are shown as individual points. (d) Relative abundance of microbial genera in tongue coating samples across groups. (e) Comparison of *Streptococcus* and *Prevotella* abundances in tongue coating samples among groups. (f) LEfSe analysis identifying differentially abundant genera and species in tongue coating samples. Taxa are color-coded by group. Statistical significance was determined using the Kruskal–Wallis test ($P < 0.05$) with a LDA score > 2.0. (g) Comparison of *Gemella, Fusobacterium*, and *Neisseria* abundances in tongue coating samples between HC and CD groups. (h) Comparison of *Prevotella oris, Prevotella denticola, Prevotella baroniae, and Gemella* abundances in tongue coating samples between HC and UC groups. (i–m) Fecal microbiota analysis. (i) PCoA based on Bray–Curtis dissimilarity showing β-diversity of fecal samples. Each point represents an individual sample; group differences were assessed by PERMANOVA ($P < 0.05$). (j, k) α-Diversity of fecal microbiota assessed using the (j) Shannon and (k) Simpson indices. One-way ANOVA revealed significant differences among groups ($P < 0.05$). Boxplot elements are defined as in (b) and (c). (l) Relative abundance of microbial genera in fecal samples across groups. (m) LEfSe analysis identifying differentially abundant fecal microbial taxa among groups, using the Kruskal–Wallis test ($P < 0.05$) and an LDA score > 2.0.

NOVA: CD vs HC, $P = 0.002$; UC vs HC, $P = 0.001$; Fig. 1(i)). Both CD and UC patients exhibited significantly reduced microbial richness and diversity compared with HCs, as reflected by decreased Shannon and Simpson indices (Figs. 1(j) and (k)), indicating a global loss of commensal bacterial complexity in IBD. At the genus level, *Prevotella* was significantly enriched in fecal samples from CD patients (Fig. 1(l)). Linear discriminant analysis (LDA) effect size (LEfSe) analysis further identified disease-specific dysbiotic signatures. CD-associated fecal microbiota was characterized by enrichment of potentially pro-inflammatory genera, including *Escherichia-Shigella*, *Veillonella*, and *Fusobacterium*, accompanied by marked depletion of beneficial commensals such as *Bifidobacterium*, *Eubacterium hallii*, and *Anaerostipes* (Fig. 1(m)). In contrast, UC fecal microbiota showed increased abundances of *Morganella*, *Erysipelatoclostridium*, *Romboutsia*, and *Flavonifractor*, along with decreased levels of *Anaerostipes*, *Eubacterium hallii*, *Bacteroides massiliensis*, and *Alistipes* (Fig. 1(m)). Collectively, these findings demonstrate that both CD and UC are associated with a shared reduction in fecal microbial diversity and a consistent depletion of key butyrate-producing taxa, despite each disease exhibiting a distinct compositional dysbiosis. This loss of short-chain fatty acid-producing bacteria may represent a common microbial mechanism contributing to impaired mucosal homeostasis in IBD.

3.2. Animal models recapitulate oral-gut microbiota dysbiosis associated with IBD

To validate the generalizability of the oral–gut microbiota dysbiosis observed in patients with IBD and to explore its potential pathogenic relevance, we examined the $TNF^{\Delta ARE}$ spontaneous enteritis mouse model [23]. Compared with WT littermate controls, $TNF^{\Delta ARE}$ mice exhibited marked alterations in microbial community structure in both fecal and tongue coating samples, as evidenced by distinct β-diversity clustering in PCoA analysis (Figs. 2(a) and (b)). Importantly, $TNF^{\Delta ARE}$ mice recapitulated several key microbial features characteristic of CD. In the intestinal compartment, $TNF^{\Delta ARE}$ mice displayed CD-like dysbiosis, including significant enrichment of *Prevotella*, particularly *Prevotellaceae* UCG-001 and *Prevotellaceae* NK3B31 (Fig. 2(c)). Concordantly, the tongue coating microbiota of $TNF^{\Delta ARE}$ mice showed increased abundance of *Streptococcus* accompanied by a depletion of *Neisseria* (Fig. 2(d)), similar to the oral microbial shifts observed in CD patients. Notably, *Prevotellaceae* NK3B31 was simultaneously enriched in both fecal and tongue coating samples from $TNF^{\Delta ARE}$ mice (Fig. 2(e)), suggesting coordinated oral–gut expansion of this taxon. *Prevotellaceae* UCG-001 was significantly increased in fecal samples and exhibited a similar increasing trend in the oral microbiota (Fig. 2(f)). Together, these findings support a potential pro-inflammatory role for specific *Prevotella* lineages across oral and intestinal niches. Consistent with these observations, LEfSe analysis identified enrichment of multiple *Prevotella* species in the gut of $TNF^{\Delta ARE}$ mice, along with a wide depletion of key commensal and short-chain fatty acid-producing genera, including *Bifidobacterium* and *Anaerostipes*. In the oral compartment, LEfSe further revealed a significant reduction in *Neisseria* abundance (Fig. 2(g)). Collectively, these results demonstrate that the $TNF^{\Delta ARE}$ model faithfully reproduces the oral–gut microbial dysbiosis observed in human IBD, supporting its utility for mechanistic studies of microbiota-driven intestinal inflammation.

3.3. Tongue coating microbiota from CD patients exacerbates colitis in mice

To directly assess the pathogenic potential of tongue coating microbiota in IBD, we transplanted tongue coating microbial communities from patients with CD or HCs into antibiotic-treated (Abx) mice, followed by induction of colitis using DSS (Fig. 3(a)). Mice colonized with CD-derived tongue coating microbiota (Abx-CD) developed significantly more severe colitis than mice receiving HC-derived microbiota (Abx-HC) or antibiotic-treated controls without transplantation (Abx), as evidenced by greater body weight loss, shortened colon length, and more pronounced histopathological damage (Figs. 3(b)–(f)). In contrast, no significant differences were observed between the Abx-HC and Abx groups, indicating that tongue coating microbiota from healthy individuals did not exacerbate intestinal inflammation. To determine whether these phenotypic differences were associated with alterations in intestinal microbial composition, we performed 16S rRNA gene sequencing of fecal samples following transplantation. PCoA revealed distinct microbial community structures among the Abx-CD, Abx-HC, and Abx groups (Fig. 3(g)), accompanied by significant differences between the Abx-CD and Abx-HC groups in α-diversity in α-diversity (Figs. 3(h) and (i)). Notably, mice receiving CD-derived tongue coating microbiota exhibited enrichment of potentially pro-inflammatory taxa, including *Klebsiella*, along with depletion of short-chain fatty acid-producing commensals such as *Akkermansia*, *Lachnoclostridium*, and *Anaerostipes*, compared with Abx-HC mice (Figs. 3(j) and (k); $P < 0.05$). These findings suggest that specific oral bacteria present in CD patients possess a selective advantage for colonization and expansion within the inflamed intestinal environment. Consistent with this notion, *Klebsiella* species, previously isolated from oral and salivary microbiota, have been shown to induce Th1 cell responses and promote intestinal inflammation [18]. In contrast, tongue coating microbiota from healthy individuals exerted minimal effects on gut microbial composition and disease severity, likely reflecting the absence of pathogenic oral taxa capable of establishing ectopic colonization in the intestine. Together, these results provide functional evidence that CD-associated tongue coating microbiota can reshape gut microbial communities and directly exacerbate colitis.

3.4 Colonization with Streptococcus vestibularis (S. vestibularis) from CD patients exacerbates colitis

Having demonstrated the pathogenic potential of the tongue coating microbiota as a whole, we next sought to identify specific oral bacterial taxa responsible for driving intestinal inflammation. From the tongue coating samples of CD patients, we successfully isolated two streptococcal species, *Streptococcus salivarius* (*S. salivarius*) and *S. vestibularis*, a genus consistently enriched in both CD patients and spontaneous enteritis ($TNF^{\Delta ARE}$) mice. Although *Prevotella* species were also enriched in tongue coating and fecal samples from CD patients, repeated attempts to isolate viable *Prevotella* strains were unsuccessful. We first evaluated the immunomodulatory capacity of the isolated *Streptococci in vitro*. Under Th1-skewing conditions, both *S. salivarius* and *S. vestibularis* significantly promoted Th1 cell differentiation, as evidenced by increased IFN-γ production, while exerting minimal effects on Th17 polarization (Figs. 4(a)–(d), Fig. S1 in Appendix A). These findings suggested a preferential role for streptococcal species in driving Th1-biased immune responses. To assess the pathogenic relevance of these observations *in vivo*, antibiotic-treated mice were colonized with *S. vestibularis* and subsequently subjected to DSS-induced colitis (Fig. 4(e)). Mice colonized with *S. vestibularis* developed markedly more severe colitis than control mice, as indicated by enhanced body weight loss, increased histopathological scores, and a significant accumulation of Th1 cells in the colonic lamina propria (Figs. 4(f)–(h); Figs. S2(a)–(d) in Appen-

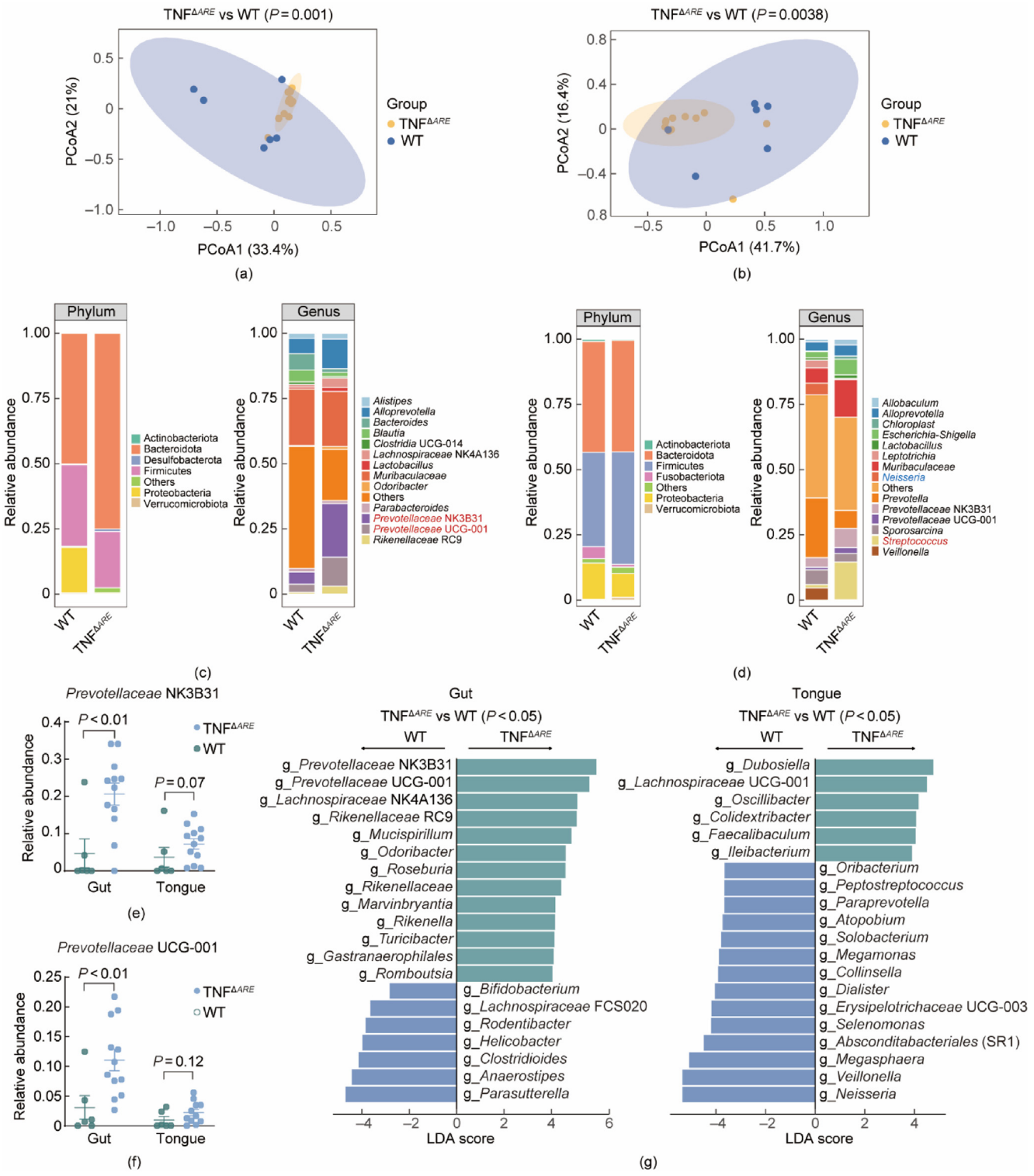

Fig. 2. Alterations in tongue coating and gut microbiota in a mouse model of spontaneous enteritis. (a, b) PCoA based on Bray–Curtis dissimilarity illustrating β-diversity of (a) fecal and (b) tongue coating microbiota in TNF$^{\Delta ARE}$ mice and WT littermate controls. Group differences were assessed by PERMANOVA ($P < 0.05$). (c, d) Relative abundance of microbial taxa at the phylum and genus levels in (c) fecal and (d) tongue coating samples from TNF$^{\Delta ARE}$ mice and controls. (e, f) Relative abundance of (e) *Prevotellaceae* NK3B31 and (f) *Prevotellaceae* UCG-001 in fecal and tongue coating samples from TNF$^{\Delta ARE}$ mice and controls. (g) LEfSe analysis identifying differentially abundant genera in the gut and tongue coating microbiota of TNF$^{\Delta ARE}$ mice compared with controls (Kruskal–Wallis test, $P < 0.05$; LDA score > 2.0). All diversity metrics were calculated using QIIME 2 (v2020.6) following rarefaction to 10 000 reads per sample. Statistical comparisons were performed using one-way ANOVA with Tukey's post hoc test (WT, $N = 6$; TNF$^{\Delta ARE}$, $N = 12$).

dix A). Notably, the proportion of IFN-γ-producing CD4$^+$ T cells was selectively increased, whereas Th17 cells were not substantially affected. The pathogenic role of *S. vestibularis* was further validated using an independent TNBS-induced colitis model (Fig. 4(i)). Consistent with the DSS model, *S. vestibularis*-colonized mice exhibited greater body weight loss, more

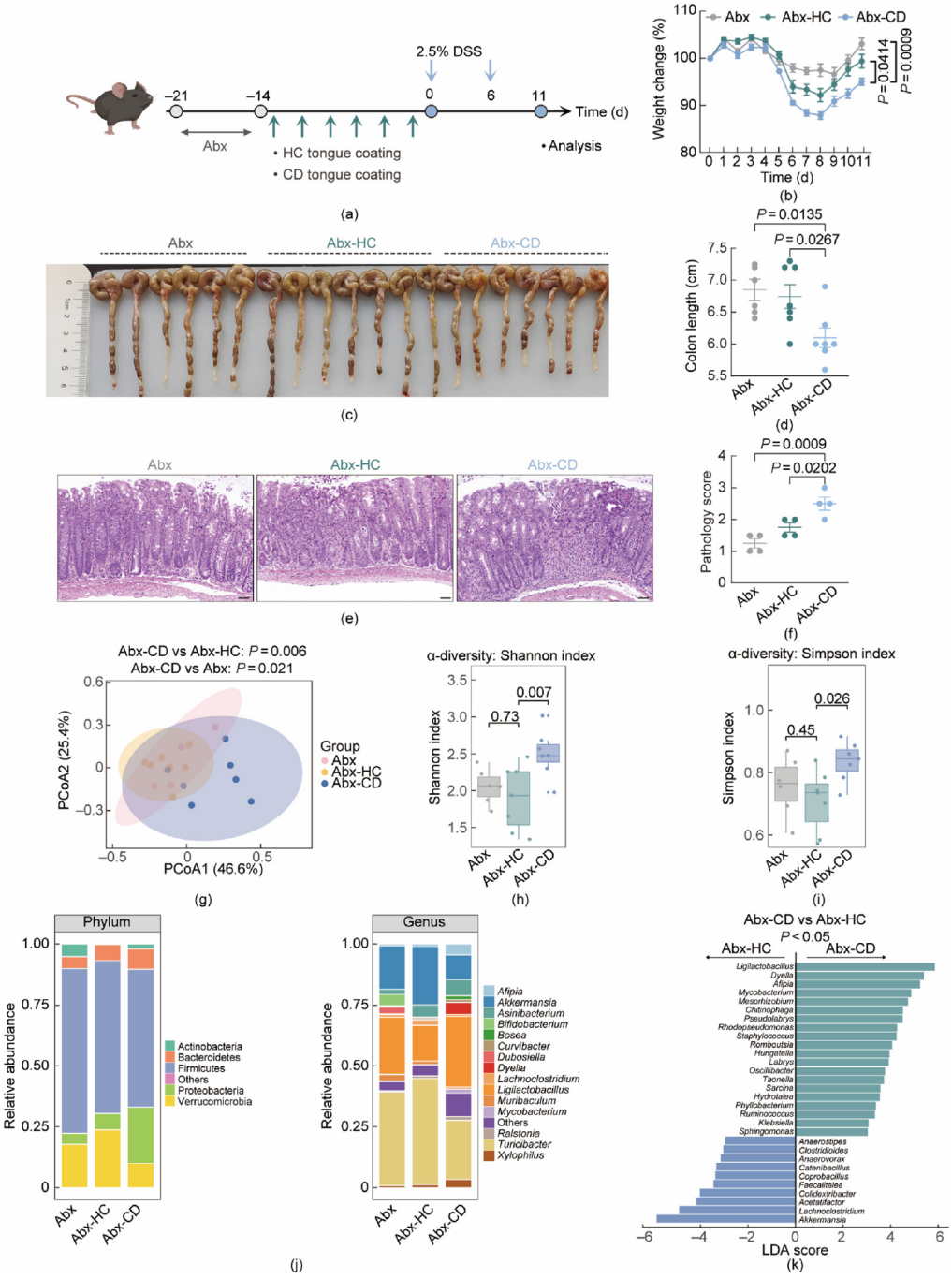

Fig. 3. Tongue coating microbiota from CD patients exacerbates DSS-induced colitis in mice. (a) Experimental schematic. Mice were treated with broad-spectrum antibiotics (Abx) for one week to deplete endogenous gut microbiota, followed by oral gavage of tongue coating microbiota from CD patients or HCs for two weeks. Colitis was then induced by administration of 2.5% (w/v) DSS in drinking water for 6 d (Abx, $N = 6$; Abx-HC and Abx-CD, $N = 7$). (b) Body weight changes monitored daily throughout the experimental period. (c, d) Representative macroscopic images of (c) colons and (d) corresponding colon lengths from each group. (e) Representative H&E-stained colon sections and (f) quantitative histological colitis scores in Abx, Abx-HC, and Abx-CD mice. Scale bars, 50 μm. (g) PCoA of fecal microbiota following tongue coating microbiota transplantation. Group differences were assessed by PERMANOVA. (h, i) α-Diversity of fecal microbiota assessed by the (h) Shannon and (i) Simpson indices. (j) Relative abundance of dominant bacterial phyla and genera accounting for 90% of the fecal microbial community across groups. (k) LEfSe analysis identifying differentially abundant genera among groups (Kruskal–Wallis test, $P < 0.05$; LDA score > 2.0). Data are presented as mean ± standard error of the mean (SEM). Statistical significance was assessed using two-tailed unpaired *t* tests (d, f) and two-way ANOVA with Tukey's post hoc test (b).

pronounced colon shortening, exacerbated histopathological injury, and significantly increased infiltration of colonic Th1 cells compared with controls (Figs. 4(j)–(l), Figs. S2(e)–(h) in Appendix A). Collectively, these findings establish a direct causal relationship between a specific CD-associated oral bacterium and intestinal immunopathology. They identify *S. vestibularis* as a potent Th1-inducing pathobiont capable of ectopic intestinal colonization and exacerbation of colitis,

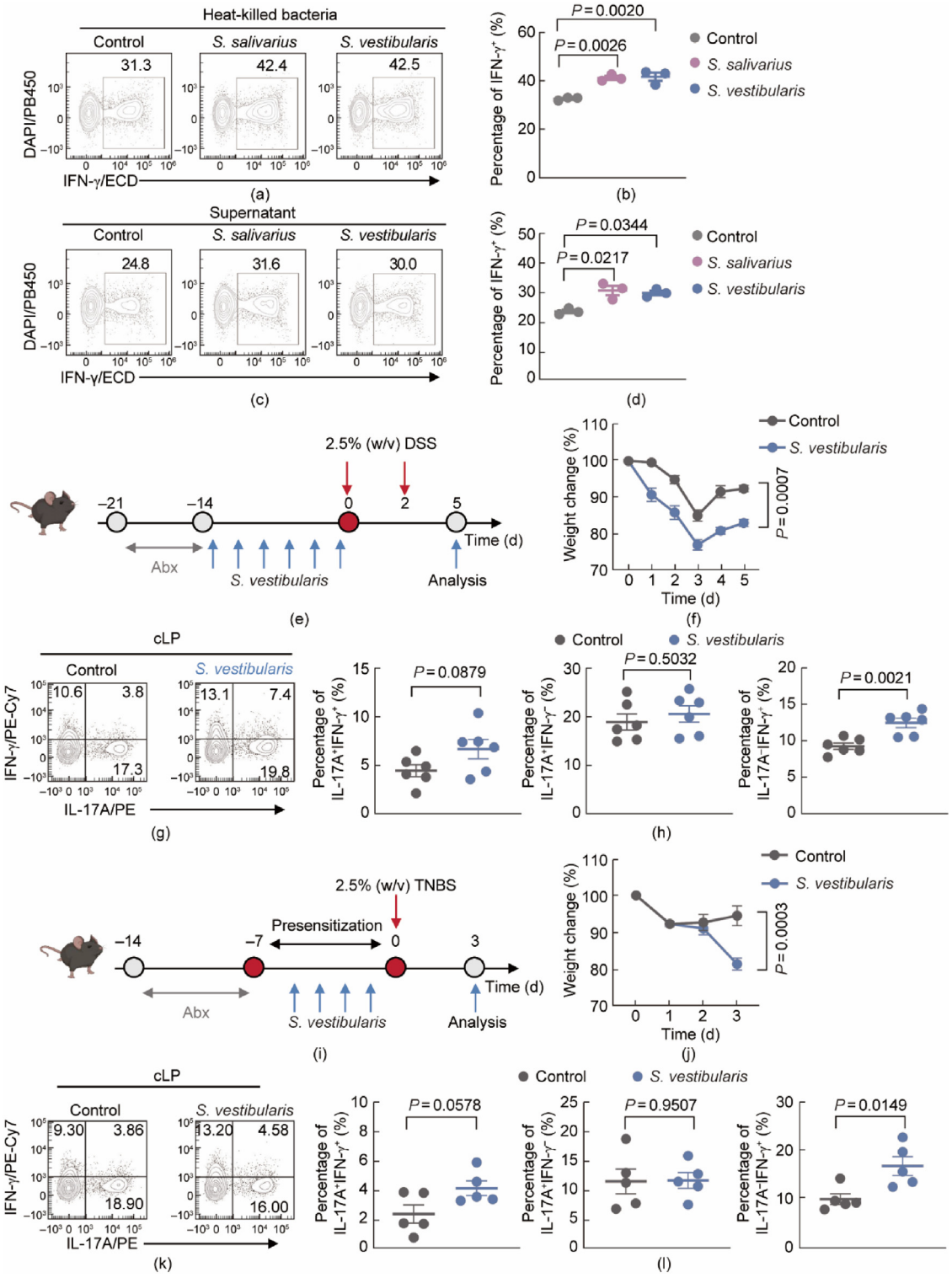

Fig. 4. Colonization with *S. vestibularis* from CD patients exacerbates experimental colitis. (a) Representative flow cytometry plots and (b) quantification of IFN-γ^+ CD4$^+$ T cells following stimulation with heat-killed *Streptococcus* species under Th1-skewing conditions. (c) Representative flow cytometry plots and (d) quantification of IFN-γ^+ CD4$^+$ T cells following stimulation with bacterial culture supernatants under Th1-skewing conditions ($N = 3$). (e) Experimental design for DSS-induced colitis. Mice were treated with broad-spectrum antibiotics (Abx) for one week, followed by oral gavage with *S. vestibularis* for two weeks prior to colitis induction using 2.5% (w/v) DSS for 2 d ($N = 6$). (f) Daily body weight changes during DSS-induced colitis. (g) Representative flow cytometry plots and (h) quantification of IL-17A$^+$IFN-γ^+, IL-17A$^+$IFN-γ^-, and IL-17A$^-$IFN-γ^+ CD4$^+$ T cells in the colonic lamina propria (cLP). (i) Experimental design for TNBS-induced colitis. Following seven days of antibiotic treatment, mice underwent epicutaneous presensitization and oral gavage with *S. vestibularis*. Colitis was induced by intrarectal administration of 2.5% (w/v) TNBS ($N = 5$). (j) Daily body weight changes during TNBS-induced colitis. (k) Representative flow cytometry plots and (l) quantification of IL-17A$^+$IFN-γ^+, IL-17A$^+$IFN-γ^-, and IL-17A$^-$IFN-γ^+ CD4$^+$ T cells in the cLP. Experiments in (a–d) were performed twice independently. Data are presented as mean ± SEM. Statistical significance was determined using two-tailed unpaired *t* tests (h, l), one-way ANOVA with Tukey's post hoc test (b, d), and two-way ANOVA with Tukey's post hoc test (f, j). PB450: pacific blue 450; ECD: energy coupled dye; cLP: colonic lamina propria; PE: phycoerythrin; Cy7: cyanine 7.

thereby implicating oral *Streptococcus* species as key contributors to the oral–gut axis in IBD.

4. Conclusions

This study provides evidence that the tongue coating microbiota serves not only as a potential diagnostic biomarker but also as a functional contributor to IBD, particularly CD. By integrating comprehensive microbial profiling with experimental validation, we demonstrate that oral–gut microbial interactions constitute a previously underappreciated pathway in IBD pathogenesis. Our findings advance mechanistic understanding of the oral–gut axis and highlight opportunities for non-invasive diagnostics and targeted microbial interventions in chronic intestinal inflammation. We identified a distinct dysbiotic signature in the tongue coating of IBD patients, characterized by enrichment of *Streptococcus*, *Prevotella*, and *Gemella*. Corresponding alterations were observed in fecal microbiota, with CD patients showing increased *Fusobacteriota* and *Prevotella*, along with depletion of butyrate-producing taxa such as *Anaerostipes* and *Eubacterium hallii*, suggesting a potential ecological linkage between oral and gut microbial communities. Although *Prevotella* is generally associated with fiber-rich diets and short-chain fatty acid (SCFA) production [30–32], several strains (e.g., *Prevotella copri*, *Prevotella intermedia*, and *Prevotella nigrescens*) have been implicated in pro-inflammatory responses, immune modulation via Th17 pathways, and diseases including periodontitis, rheumatoid arthritis, and IBD [33–40]. This dualistic role highlights the importance of future studies to resolve strain-level functions and their context-specific impacts on host health [30]. The biological relevance of these oral–gut microbial alterations was further supported in a spontaneous model of chronic intestinal inflammation. $TNF^{\Delta ARE}$ mice recapitulated key microbial features observed in CD patients, including enrichment of *Streptococcus* in the tongue coating and selective *Prevotella* strains in both oral and gut niches, reinforcing the plausibility of oral-derived bacteria in driving intestinal inflammation. Functionally, we established causality through oral microbiota transplantation experiments. Mice receiving tongue coating microbiota from CD patients developed more severe DSS-induced colitis than those receiving HC microbiota. This was accompanied by expansion of pro-inflammatory genera such as *Klebsiella* [41–43], and depletion of beneficial SCFA-producing taxa, including *Akkermansia* and *Anaerostipes* [44–46]. These results align with previous evidence that oral pathobionts can modulate intestinal immunity and exacerbate chronic gut inflammation. Mechanistically, we show that *Streptococcus* strains isolated from CD patients promote Th1 polarization *in vitro* and aggravate colitis *in vivo*, providing direct support for a pathogenic role of oral *Streptococci* in gut inflammation. Previous studies have linked specific *Streptococcus* species to intestinal or systemic pathology: *Streptococcus pneumoniae* disrupts gut microbial homeostasis and triggers Toll–like receptor (TLR)-mediated systemic inflammation; *Streptococcus mutans* can exacerbate dysbiosis following translocation [47–49]; *Streptococcus gallolyticus* promotes colorectal cancer and inflammation via IL-1β/Th17 signaling [50]; and commensal oral *Streptococci* such as *Streptococcus sanguinis* and *Streptococcus oralis* impair epithelial barrier integrity [51]. Accordingly, our identification of pathogenic *S. vestibularis* in CD patients highlights that a consortium of oral *Streptococci* may cooperatively fuel intestinal inflammation through diverse immunological mechanisms, establishing a mechanistic relationship between oral microbiota and CD pathogenesis.

While our study provides novel insights into the role of tongue coating microbiota in IBD, several limitations should be acknowledged. First, focusing exclusively on tongue coating samples may not fully capture the complexity of oral–gut axis dysbiosis, as the oral cavity comprises multiple distinct ecological niches (e.g., subgingival crevices and saliva) with specialized microbial communities that may differentially influence intestinal inflammation [52–54]. Future studies employing multi-niche sampling strategies are needed to comprehensively define the oral microbiome's contribution to IBD pathogenesis. Methodologically, we faced challenges in isolating oral *Prevotella* strains, which precluded direct functional validation of their proposed pro-inflammatory role. Additionally, although our mouse models recapitulated key features of human IBD, inherent interspecies differences in host–microbe interactions warrant caution when extrapolating these findings to humans. From a clinical perspective, inconsistent documentation of oral manifestations within our cohort limited our ability to stratify patients based on this potential confounder. It remains possible that the observed oral dysbiosis reflects local oral inflammation, which may in turn influence gut homeostasis. To address these gaps, future work should integrate multi-niche oral sampling with shotgun metagenomics to achieve strain-level resolution, enhanced culturing techniques for functional characterization of specific isolates, concurrent host immune profiling, and systematic oral phenotyping. Such integrative approaches will be essential for establishing causality and elucidating the precise mechanisms through which oral microbes contribute to intestinal inflammation in IBD.

CRediT authorship contribution statement

Yanqing Wang: Writing – original draft, Methodology, Investigation, Formal analysis, Data curation, Conceptualization. **Qian Xu:** Software, Methodology, Formal analysis, Data curation. **Jingyuan Wang:** Software, Methodology, Data curation, Conceptualization. **Meng Xue:** Methodology. **Honghong Liu:** Supervision, Resources. **Yifei Yang:** Software, Methodology, Formal analysis, Data curation. **Chao Ye:** Resources. **Shuling Wang:** Resources. **Gerong Zhang:** Writing – review & editing, Validation, Project administration, Conceptualization. **Wenrui Guo:** Resources. **Wei Jiang:** Resources. **Eran Elinav:** Supervision, Resources, Project administration, Funding acquisition, Conceptualization. **Shu Zhu:** Writing – review & editing, Supervision, Resources, Project administration, Funding acquisition, Conceptualization. **Guorong Zhang:** Writing – review & editing, Validation, Project administration, Conceptualization.

Declaration of competing interest

The authors declare that they have no known competing financial interests or personal relationships that could have appeared to influence the work reported in this paper.

Acknowledgments

This work was supported by grants from the National Key Research and Development Program of China (2020YFA0509101 to Wei Jiang), the National Natural Science Foundation of China (82061148013 to Shu Zhu and 32300741 to Guorong Zhang), the fellowship of China National Postdoctoral Program for Innovative Talents (BX20230341 to Guorong Zhang), the fellowship of China Postdoctoral Science Foundation (2020M682052 to Yanqing Wang. and 2022M723054 to Guorong Zhang), and the Fundamental Research Funds for the Central Universities (WK9990000162 to Guorong Zhang).

We would like to express our gratitude to the medical staff of the Department of Gastroenterology, Department of Stomatology, Health Examination Management Center, and Endoscopy Center at the First Affiliated Hospital of University of Science and Technol-

ogy of China, for their valuable assistance. We also extend our sincere thanks to all the participants for their participation and support.

Appendix A. Supplementary data

Supplementary data to this article can be found online at https://doi.org/10.1016/j.eng.2026.02.016.

References

[1] Loftus Jr EV. Clinical epidemiology of inflammatory bowel disease: incidence, prevalence, and environmental influences. Gastroenterology 2004;126(6):1504–17.
[2] Molodecky NA, Soon IS, Rabi DM, Ghali WA, Ferris M, Chernoff G, et al. Increasing incidence and prevalence of the inflammatory bowel diseases with time, based on systematic review. Gastroenterology 2012;142(1):46–54.e42. quiz e30.
[3] Bouhuys M, Lexmond WS, van Rheenen PF. Pediatric inflammatory bowel disease. Pediatrics 2023;151(1):e2022058037.
[4] Ng SC, Tang W, Ching JY, Wong M, Chow CM, Hui AJ, the Asia–Pacific Crohn's and Colitis Epidemiologic Study (ACCESS) Study Group, et al. Incidence and phenotype of inflammatory bowel disease based on results from the Asia–Pacific Crohn's and Colitis Epidemiology Study. Gastroenterology 2013;145(1):158–165.e2.
[5] Sturm A, Maaser C, Calabrese E, Annese V, Fiorino G, Kucharzik T, the European Crohn's and Colitis Organisation (ECCO) and the European Society of Gastrointestinal and Abdominal Radiology (ESGAR), et al. ECCO–ESGAR guideline for diagnostic assessment in IBD part 2: IBD scores and general principles and technical aspects. J Crohns Colitis 2019;13(3):273–84.
[6] Aziz I, Simrén M. The overlap between irritable bowel syndrome and organic gastrointestinal diseases. Lancet Gastroenterol Hepatol 2021;6(2):139–48.
[7] Federici S, Kredo-Russo S, Valdés-Mas R, Kviatcovsky D, Weinstock E, Matiuhin Y, et al. Targeted suppression of human IBD-associated gut microbiota commensals by phage consortia for treatment of intestinal inflammation. Cell 2022;185(16):2879–2898.e24.
[8] Zhang W, Lyu M, Bessman NJ, Xie Z, Arifuzzaman M, Yano H, the JRI Live Cell Bank, et al. Gut-innervating nociceptors regulate the intestinal microbiota to promote tissue protection. Cell 2022;185(22):4170–4189.e20.
[9] Sun D, Bai R, Zhou W, Yao Z, Liu Y, Tang S, et al. Angiogenin maintains gut microbe homeostasis by balancing α-Proteobacteria and Lachnospiraceae. Gut 2021;70(4):666–76.
[10] Mitsialis V, Wall S, Liu P, Ordovas-Montanes J, Parmet T, Vukovic M, the Boston Children's Hospital Inflammatory Bowel Disease Center, the Brigham and Women's Hospital Crohn's and Colitis Center, et al. Single-cell analyses of colon and blood reveal distinct immune cell signatures of ulcerative colitis and Crohn's disease. Gastroenterology 2020;159(2):591–608.e10.
[11] Manichanh C, Rigottier-Gois L, Bonnaud E, Gloux K, Pelletier E, Frangeul L, et al. Reduced diversity of faecal microbiota in Crohn's disease revealed by a metagenomic approach. Gut 2006;55(2):205–11.
[12] Dickson I. Gut microbiota: oral bacteria: a cause of IBD? Nat Rev Gastroenterol Hepatol 2018;15(1):4–5.
[13] Ray K. The oral–gut axis in IBD. Nat Rev Gastroenterol Hepatol 2020;17(9):532.
[14] Xiao E, Mattos M, Vieira GHA, Chen S, Corrêa JD, Wu Y, et al. Diabetes enhances IL-17 expression and alters the oral microbiome to increase its pathogenicity. Cell Host Microbe 2017;22(1):120–128.e4.
[15] Zhen W, Wang Z, Wang Q, Sun W, Wang R, Zhang W, et al. Cardiovascular disease therapeutics via engineered oral microbiota: applications and perspective. iMeta 2024;3(3):e197.
[16] Shu J, Yu H, Ren X, Wang Y, Zhang K, Tang Z, et al. Role of salivary glycopatterns for oral microbiota associated with gastric cancer. Int J Biol Macromol 2022;209(Pt A):1368–78.
[17] Kitamoto S, Nagao-Kitamoto H, Jiao Y, Gillilland 3rd MG, Hayashi A, Imai J, et al. The intermucosal connection between the mouth and gut in commensal pathobiont-driven colitis. Cell 2020;182(2):447–462.e14.
[18] Atarashi K, Suda W, Luo C, Kawaguchi T, Motoo I, Narushima S, et al. Ectopic colonization of oral bacteria in the intestine drives TH1 cell induction and inflammation. Science 2017;358(6361):359–65.
[19] van Tornout M, Dadamio J, Coucke W, Quirynen M. Tongue coating: related factors. J Clin Periodontol 2013;40(2):180–5.
[20] Chen H, Li Q, Li M, Liu S, Yao C, Wang Z, et al. Microbial characteristics across different tongue coating types in a healthy population. J Oral Microbiol 2021;13(1):1946316.
[21] Yuan L, Yang L, Zhang S, Xu Z, Qin J, Shi Y, et al. Development of a tongue image-based machine learning tool for the diagnosis of gastric cancer: a prospective multicentre clinical cohort study. eClinicalMedicine 2023;57:101834.
[22] Bernstein CN, Fried M, Krabshuis JH, Cohen H, Eliakim R, Fedail S, et al. World gastroenterology organization practice guidelines for the diagnosis and management of IBD in 2010. Inflamm Bowel Dis 2010;16(1):112–24.
[23] Chakraborty R, Maltz MR, Del Castillo D, Tandel PN, Messih N, Anguiano M, et al. Selective targeting of tumour necrosis factor receptor 1 induces stable protection from Crohn's-like ileitis in $TNF^{\Delta ARE}$ mice. J Crohns Colitis 2022;16(6):978–91.
[24] Routy B, Le Chatelier E, Derosa L, Duong CPM, Alou MT, Daillère R, et al. Gut microbiome influences efficacy of PD-1-based immunotherapy against epithelial tumors. Science 2018;359(6371):91–7.
[25] Wirtz S, Neufert C, Weigmann B, Neurath MF. Chemically induced mouse models of intestinal inflammation. Nat Protoc 2007;2(3):541–6.
[26] Tanoue T, Morita S, Plichta DR, Skelly AN, Suda W, Sugiura Y, et al. A defined commensal consortium elicits CD8 T cells and anti-cancer immunity. Nature 2019;565(7741):600–5.
[27] Chen C, Zhang W, Zhou T, Liu Q, Han C, Huang Z, et al. Vitamin B5 rewires Th17 cell metabolism via impeding PKM2 nuclear translocation. Cell Rep 2022;41(9):111741.
[28] Alexander M, Ang QY, Nayak RR, Bustion AE, Sandy M, Zhang B, et al. Human gut bacterial metabolism drives Th17 activation and colitis. Cell Host Microbe 2022;30(1):17–30.e9.
[29] Dieleman LA, Palmen MJ, Akol H, Bloemena E, Peña AS, Meuwissen SG, et al. Chronic experimental colitis induced by dextran sulphate sodium (DSS) is characterized by Th1 and Th2 cytokines. Clin Exp Immunol 1998;114(3):385–91.
[30] Li J, Zhao F, Wang Y, Chen J, Tao J, Tian G, et al. Gut microbiota dysbiosis contributes to the development of hypertension. Microbiome 2017;5(1):14.
[31] Li YJ, Chen X, Kwan TK, Loh YW, Singer J, Liu Y, et al. Dietary fiber protects against diabetic nephropathy through short-chain fatty acid-mediated activation of g protein-coupled receptors GPR43 and GPR109a. J Am Soc Nephrol 2020;31(6):1267–81.
[32] Rinott E, Meir AY, Tsaban G, Zelicha H, Kaplan A, Knights D, et al. The effects of the Green-Mediterranean diet on cardiometabolic health are linked to gut microbiome modifications: a randomized controlled trial. Genome Med 2022;14(1):29.
[33] Qi Y, Zang SQ, Wei J, Yu HC, Yang Z, Wu HM, et al. High-throughput sequencing provides insights into oral microbiota dysbiosis in association with inflammatory bowel disease. Genomics 2021;113(1 Pt 2):664–76.
[34] Abdelbary MMH, Hatting M, Bott A, Dahlhausen A, Keller D, Trautwein C, et al. The oral–gut axis: salivary and fecal microbiome dysbiosis in patients with inflammatory bowel disease. Front Cell Infect Microbiol 2022;12:1010853.
[35] Nii T, Maeda Y, Motooka D, Naito M, Matsumoto Y, Ogawa T, et al. Genomic repertoires linked with pathogenic potency of arthritogenic *Prevotella copri* isolated from the gut of patients with rheumatoid arthritis. Ann Rheum Dis 2023;82(5):621–9.
[36] Zhao Y, Feng Y, Ye Q, Hu J, Feng Y, Ouyang Z, et al. The oral microbiome in young women at different stages of periodontitis: *Prevotella* dominant in stage iii periodontitis. Front Cell Infect Microbiol 2022;12:1047607.
[37] Braga RR, Carvalho MA, Bruña-Romero O, Teixeira RE, Costa JE, Mendes EN, et al. Quantification of five putative periodontal pathogens in female patients with and without chronic periodontitis by real-time polymerase chain reaction. Anaerobe 2010;16(3):234–9.
[38] Shah HN, Collins DM. *Prevotella*, a new genus to include *Bacteroides melaninogenicus* and related species formerly classified in the genus *Bacteroides*. Int J Syst Bacteriol 1990;40(2):205–8.
[39] Wu TT, Xiao J, Sohn MB, Fiscella KA, Gilbert C, Grier A, et al. Machine learning approach identified multi-platform factors for caries prediction in child-mother dyads. Front Cell Infect Microbiol 2021;11:727630.
[40] Plummer EL, Sfameni AM, Vodstrcil LA, Danielewski JA, Murray GL, Fehler G, et al. *Prevotella* and *Gardnerella* are associated with treatment failure following first-line antibiotics for bacterial vaginosis. J Infect Dis 2023;228(5):646–56.
[41] Newman NK, Zhang Y, Padiadpu J, Miranda CL, Magana AA, Wong CP, et al. Reducing gut microbiome-driven adipose tissue inflammation alleviates metabolic syndrome. Microbiome 2023;11(1):208.
[42] Seki D, Mayer M, Hausmann B, Pjevac P, Giordano V, Goeral K, et al. Aberrant gut–microbiota–immune–brain axis development in premature neonates with brain damage. Cell Host Microbe 2021;29(10):1558–1572.e6.
[43] Gong J, Yu J, Yin S, Ke J, Wu J, Liu C, et al. Mesenteric adipose tissue-derived *Klebsiella variicola* disrupts intestinal barrier and promotes colitis by type vi secretion system. Adv Sci 2023;10(12):e2205272.
[44] De Vos WM, Nguyen Trung M, Davids M, Liu G, Rios-Morales M, Jessen H, et al. Phytate metabolism is mediated by microbial cross-feeding in the gut microbiota. Nat Microbiol 2024;9(7):1812–27.
[45] Bui TPN, Mannerås-Holm L, Puschmann R, Wu H, Troise AD, Nijsse B, et al. Conversion of dietary inositol into propionate and acetate by commensal *Anaerostipes* associates with host health. Nat Commun 2021;12(1):4798.
[46] Palmnäs-Bédard MSA, Costabile G, Vetrani C, Åberg S, Hjalmarsson Y, Dicksved J, et al. The human gut microbiota and glucose metabolism: a scoping review of key bacteria and the potential role of SCFAs. Am J Clin Nutr 2022;116(4):862–74.
[47] Ling J, Hryckowian AJ. Re-framing the importance of group B *Streptococcus* as a gut-resident pathobiont. Infect Immun 2024;92(9):e0047823.
[48] Schmidt TS, Hayward MR, Coelho LP, Li SS, Costea PI, Voigt AY, et al. Extensive transmission of microbes along the gastrointestinal tract. eLife 2019;8:42693.
[49] Kojima A, Nakano K, Wada K, Takahashi H, Katayama K, Yoneda M, et al. Infection of specific strains of *Streptococcus mutans*, oral bacteria, confers a risk of ulcerative colitis. Sci Rep 2012;2:332.
[50] Périchon B, Cokelaer T, Teh WK, du Merle L, Ma L, Touchon M, et al. Colorectal cancer-associated *Streptococcus gallolyticus*: a hidden diversity expose. J Bacteriol 2025;207(9):e0023025.

[51] Okahashi N, Sumitomo T, Nakata M, Sakurai A, Kuwata H, Kawabata S. Hydrogen peroxide contributes to the epithelial cell death induced by the oral mitis group of streptococci. PLoS One 2014;9(1):e88136.
[52] Proctor DM, Shelef KM, Gonzalez A, Davis CL, Dethlefsen L, Burns AR, et al. Microbial biogeography and ecology of the mouth and implications for periodontal diseases. Periodontol 2000 2020,;82(1):26–41.
[53] Carda-Diéguez M, Rosier BT, Lloret S, Llena C, Mira A. The tongue biofilm metatranscriptome identifies metabolic pathways associated with the presence or absence of halitosis. NPJ Biofilms Microbiomes 2022;8(1):100.
[54] Moradi J, Berggreen E, Bunæs DF, Bolstad AI, Bertelsen RJ. Microbiome composition and metabolic pathways in shallow and deep periodontal pockets. Sci Rep 2025;15(1):12926.